MDPI

Article

Oblique Detonation Wave Control with O_3 and H_2O_2 Sensitization in Hypersonic Flow

Ashish Vashishtha [1,*], Snehasish Panigrahy[2], Dino Campi[1], Dean Callaghan [3], Cathal Nolan [1] and, Ralf Deiterding [4]

[1] Department of Aerospace & Mechanical Engineering, South East Technological University (SETU), Carlow Campus, R93 V960 Ireland;
[2] Department of Energy Science and Engineering, Indian Institute of Technology Delhi, 110016 India;
[3] The Center for Research and Enterprise in Engineering (engCORE), South East Technological University (SETU), Carlow Campus, R93 V960 Ireland;
[4] Aerodynamics and Flight Mechanics Research Group, University of Southampton, Boldrewood Innovation Campus, Southampton, SO16 7QF, United Kingdom
* Correspondence: ashish.vashishtha@setu.ie

Abstract: This numerical study investigates the effects of adding a small amount of ignition promoters for controlling the wedge induced oblique shock wave (OSW) to oblique detonation wave (ODW) transition in a premixed hydrogen air mixture at hypersonic speeds. The time dependent two-dimensional compressible Euler equations for multiple thermally perfect species with a reactive source term are solved using adaptive mesh refinement and detailed chemical kinetics. The wedge with a fixed angle 26° exhibits abrupt to smooth transitions for freestream Mach numbers 7 - 9 (speeds 2.8 -3.2 km/s) at a pressure of 20 kPa and temperature of 300K. The small amount (1000 PPM by vol.) of H_2O_2 and O_3 is found to be effective in significantly reducing the initiation length for oblique detonation transition for all the Mach numbers, which suggests a practical approach to increase the operating flight range for oblique detonation wave engine with a finite length wedge. At Mach number 8, the abrupt OSW to ODW transition turns towards smooth transition with a small amount of H_2O_2 and O_3 addition. Comparatively, O_3 addition was found effective in reducing the ODW initiation length by promoting reactivity behind even a weaker oblique shock at low Mach number 7 for abrupt transition, while H_2O_2 addition was more effective than O_3 at high Mach numbers 8 and 9 during smooth transition. The maximum 73 % and 80 % reduction in initiation length of ODW was observed with 10000 PPM H_2O_2 and O_3 addition, respectively, during abrupt OSW to ODW transition at Mach 7.

Keywords: Schramjet, Oblique Detonation Wave, Hypersonic Flow, Detailed Chemical Kinetics, Fuel-sensitization

Citation: Vashishtha, A.; Panigrahy, S.; Campi, D.; Callaghan, D.; Nolan, C.; Deiterding, R. Oblique Detonation Wave Control with O_3 and H_2O_2 Sensitization in Hypersonic Flow. *Energies* **2022**, *1*, 0. https://doi.org/

Received:
Accepted:
Published:

1. Introduction

Between two combustion modes: deflagration and detonation [1], detonation based combustion systems have been found to achieve higher heat release rate as well as higher thermodynamic efficiency than the deflagration based systems. Other advantages such as simpler design and shorter combustor length makes a detonation based combustor system, an ideal candidate to integrate with future hypersonic transport vehicles. In recent decades, Kailasanath [2] and Wolanski [3] have reviewed the progress of detonation based propulsion systems, mainly pulse detonation engine (PDE), rotatory detonation engine (RDE) and Oblique detonation wave engine (ODWE), also referred as shock induced combustion ramjet (or shcramjet). Among these three detonation based propulsive systems, the Oblique detonation wave engine (ODWE) concept has simplest design and can be easily integrated in a scramjet engine configuration. It requires a wedge in supersonic premixed stream of fuel-air mixture, which can establish a compression wave as oblique shock wave.

Sufficient compression provided by oblique shock can ignite fuel-air mixture and may turn it in standing or propagating detonation wave [4], which can be further accelerated through the nozzle. The main challenge in realizing ODWE is to initiate detonation at a desired location on the finite wedge and stabilize it for a range of flight Mach numbers. In preliminary studies, reactive Rankine-Hugoniot analysis [5,6] is used by approximating ODW as an oblique shock wave (OSW) coupled with an instantaneous heat release to understand the stable oblique detonation wave formation. In order to obtain a stable oblique detonation wave for a given Mach number and premixed mixture, the deflection angle should be in the range of ($\theta_{CJ} < \theta < \theta_{detach}$), corresponding to weak overdriven ODW. When the high-speed (supersonic or hypersonic) premixed fuel-air mixture (at a given freestream pressure P_∞ & temperature T_∞) encounters the flow deflection due to the wedge, the oblique shock forms at the tip of the wedge. The oblique shock compresses the fuel-air mixture and at appropriate compression (combination of θ with $\theta_{CJ} < \theta < \theta_{detach}$ and M_∞), the oblique shock will transit into oblique detonation wave through two mechanisms: abrupt transition and smooth transition [7]. The abrupt transition consists of oblique shock with a non-reactive initiation zone, deflagration wave and an oblique detonation wave forming a triple point [4,8,9]. In contrast, smooth transition occurs with curved shock at high Mach numbers with a requirement for a low activation energy condition. Figueria et al. [10] have proposed that the criteria depends on the ratio of induction time (τ_i) and total reaction time (τ_r) to distinguish between abrupt and smooth transition and suggested that abrupt transition occur when $\tau_i/\tau_r \to 1$, whereas smooth transition occur when $\tau_i/\tau_r \to 0$. Teng et al. [11] have observed various shock pattern at the end of the initiation zone such as $\lambda-$, $X-$, and $Y-$ shaped shock waves all through abrupt transition. Zhang et al. [12] have observed change in abrupt and smooth transitions by changing the deflection angle numerically. Teng et al. [13] have found that the initiation length and structure is highly dependent on freestream Mach number and less dependent on pressure. Gao et al. [14] have found that Argon dilution of more than 70 % will lead to an abrupt to smooth transition for H_2- Air mixture at a given wedge angle and hypersonic Mach number. From the above discussion, it is understood that OSW to ODW transition through abrupt or smooth mechanism can be controlled with three controlling parameters: inflow Mach number, wedge angle and chemical kinetics.

For practical purposes, it may be required to adjust the deflection angle for a finite length of wedge in order to achieve stable oblique detonation wave within its length for given flight Mach number. Miao et al. [15] suggested that smooth transition provides stable and disturbance resistivity for ODW rather than an abrupt transition pattern. It is also desirable to achieve the transition near to the starting point of the wedge to achieve reduced passage height for integration of ODWE. The current study proposes to manipulate the OSW to ODW transition by altering the chemical kinetics for a H_2- Air premixed fuel air mixture by adding ignition promoters such as H_2O_2 and O_3 in order to control the oblique detonation wave formation on a finite length wedge. Magzamov et al. [16] have shown that small amount of these additives can reduce the induction zone length significantly through ZND-calculations, due to the production of O atom and OH radical respectively. Recently, Crane et al. [17] through experimental studies with O_3 addition and Kumar et al. [18] through ZND calculations for H_2O_2 and O_3 have suggested that using a moderate amount of these ignition promoter can alter only chemical kinetic effect without changing the gasdynamic effects. The effectiveness of both ignition promoters H_2O_2 and O_3 has been well understood on fundamental gaseous detonation phenomenon using theoretical and experimental studies. The applications and effects of these ignition promoters on detonation-based propulsion system has never been studied in the literature to the authors knowledge. Previous studies related to oblique detonation wave have researched effect of inert gas dilutions [14,19,20]. The novelty and motivation of current study to utilize these ignition promoters for oblique detonation wave system to increase ODWE operable flight Mach number range for a finite length wedge.

In past literature, the experimental studies for ODW formation are mainly performed by shooting hypervelocity projectile into premixed combustible mixture [8,21] , which can only provide instantaneous detonation wave structure. Using the wedge into a shock tube facility [4,22] will provide another option for experiments, but upstream propagation of detonation wave through boundary layer poses issue of unstart [23] at various in-flow parameters and mixture conditions in confined channel. Hence, many numerical studies have been performed in past decade to understand the formation and transition of ODW and the operating range for stable ODW. Li et al. [24] had obtained stable ODW with non-reactive oblique shock wave (initiation zone), deflagration waves, tripple point, and oblique detonation using numerical simulations, which was confirmed by experimental studies by Viguier et al. [4]. This has been considered standard features for many numerical studies. The previous numerical studies [10,25,26] show that the viscosity and boundary layer have negligible effect on oblique detonation structure. With this motivation, this study uses two-dimensional inviscid numerical simulation for stabilizing the (finite length) wedge induced oblique detonation wave in premixed H_2- Air mixture with equivalence ratio 1 using detailed chemical kinetics. The abrupt and smooth transition patterns are obtained by varying the hypersonic inflow Mach number. Furthermore a moderate amount of H_2O_2 as well as O_3 are added individually to investigate their effect on oblique shock to detonation wave transition patterns. The overall objectives of the study are to: 1) numerically investigate the efficacy of ignition promoters H_2O_2 and O_3 to control of oblique detonation wave patterns and formation on finite length wedge, 2) understand the mechanism of control by quantifying the amount of additives with respect to change in initiation length of ODW formation.

2. Numerical Method

In this study, the Adaptive Mesh Refinement Object-oriented C++ (AMROC) [27–29] based on the Structured Adaptive Mesh Refinement (SAMR) solver was used with a detailed reaction model, which has been efficiently used for various shock induced combustion studies and detonation based simulation problems [15,30,31]. In various numerical studies, AMROC has been successfully used for ODW simulations with two-step mechanism [32–34] as well with detailed chemical kinetics [15]. In the current study, the simulations are performed by solving two-dimensional time-dependent compressible reactive multi-species Euler equations with detailed chemical kinetics for various incoming flows. The equations and formulation are shown below [27,31]:

$$\frac{\partial \mathbf{U}}{\partial t} + \frac{\partial \mathbf{F}}{\partial x} + \frac{\partial \mathbf{G}}{\partial y} = \mathbf{S} \tag{1}$$

where conservative state vector $\mathbf{U}$, flux vectors $\mathbf{F}$, $\mathbf{G}$ and $\mathbf{Z}$ and source term $\mathbf{S}$ are defined below:

$$\mathbf{U} = \begin{Bmatrix} \rho_1 \\ \vdots \\ \rho_n \\ \rho u \\ \rho v \\ e \end{Bmatrix}, \quad \mathbf{F} = \begin{Bmatrix} \rho_1 u \\ \vdots \\ \rho_n u \\ \rho u^2 + p \\ \rho uv \\ u(e+p) \end{Bmatrix},$$

$$\mathbf{G} = \begin{Bmatrix} \rho_1 v \\ \vdots \\ \rho_n v \\ \rho v^2 + p \\ \rho uv \\ v(e+p) \end{Bmatrix}, \quad \mathbf{S} = \begin{Bmatrix} \dot{\omega_1} \\ \vdots \\ \dot{\omega_n} \\ 0 \\ 0 \\ 0 \end{Bmatrix} \tag{2}$$

Total Density:

$$\rho = \sum_{i=1}^{n} \rho_i \tag{3}$$

Energy:

$$e = \rho h - p + \frac{1}{2}\rho(u^2 + v^2) \tag{4}$$

Specific Enthalpy:

$$h = \sum_{i=1}^{n} \frac{\rho_i h_i}{\rho} \tag{5}$$

Equation of State:

$$p = \sum_{i=1}^{n} \rho_i \frac{R}{w_i} T \tag{6}$$

in which, the source term $\dot{\omega}_i$ is the specific mass production rate of each species, which depends on the forward and backward reaction rates from the detailed chemical reaction mechanism used. w_i is the molecular weight of each species, R is the universal gas constant and T is the local temperature. The hydrogen-air combustion as well as the H_2O_2 addition calculations use 12 species 34 reaction detailed chemical kinetic mechanism for hydrogen-air detonation, which was derived from Westbrook et al. [35]. However, simulations involving O_3 addition has been modelled by adding Princeton Ozone submodel [36] to the Westbrook H_2-Air Mechanism with total 15 species with 46 reactions. This study uses chemistry module of AMROC solver, which assumes thermodynamic equilibrium temperature to estimate mixture properties and reactive source terms. The thermodynamic non-equilibrium effects (multi-temperature model) at hypersonic speeds is not considered at this stage, which will require to develop completely different solver (e.g., based on Mutation++) with integration of dissociation chemistry [37,38]. Shi et al. [39] suggested that the choice of temperature to estimate reactive source term in non-equilibrium gaseous detonation can lead to discrepancy in estimating detonation cell-size in propagating detonation. The AMROC solver decouples the hydrodynamic transport and chemical reactions numerically by utilizing a time-operator splitting approach or method of fractional steps [28]. In the current solver, Godunov splitting is adopted for decoupling and the second-order accurate MUSCL-TVD finite volume method (FVM) is used for the convective flux discretization. A hybrid Roe-HLL Riemann solver is used for the construction of the inter-cell numerical upwind fluxes, while the min-mod limiter is applied with the MUSCL reconstruction to construct a second-order method in space. The second-order accurate MUSCL-Hancock technique is adopted for time integration. The dynamic time stepping is used for all simulations by using the target CFL number as 0.95 with minimum time-step as 1×10^{-10} s. The structured automatic mesh refinement (SAMR) method based on various flow parameters was utilized here, which has low numerical diffusion in highly refined region. The details of the computation domain, boundary and initial conditions, solution procedure as well as the grid independence solution will be discussed in the following subsections.

2.1. Computational Domain

The computational domain with dimension 5 × 6 cm is shown in Fig. 1, which consists of a wedge with a fixed deflection angle $\theta = 26°$. The wedge tip starts at $X = 0.0$ and the inlet and outlet boundaries kept at X = -0.2 cm and 4.8 cm, respectively. It was expected that the oblique shock wave will establish at the tip of the wedge, and transit to an oblique detonation wave at the appropriate distance. The polar curve analysis [5] shows that for a given Mach number and fuel-air mixture, if the detonation wave solution exists, it forms higher angle than the oblique shock wave.

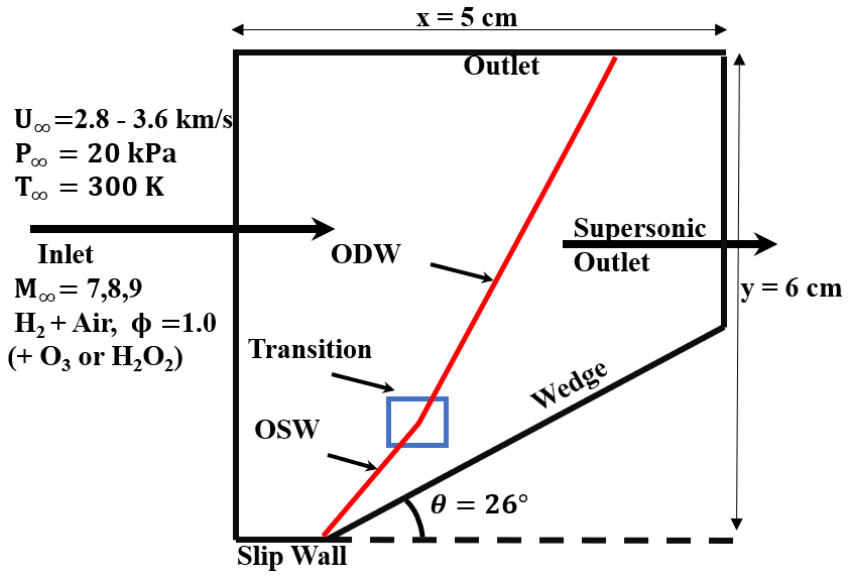

Figure 1. Computation domain & boundary conditions

Table 1. Boundary Condition & Flow Properties

Description	Value
Freestream Mach Number (M_∞)	7, 8, 9
Freestream Speed (V_∞)	2.8-3.6 km/s
Freestream Pressure (P_∞)	20 kPa
Freestream Temperature (T_∞)	300 K
H_2-Air Equivalence Ratio (ϕ)	1.0
Deflection Angle (θ)	26.0°
M_{CJ} (No Additive)	4.75
CJ Speed	1940.09 m/s (No Additive)
	1921.37 m/s (10000 PPM H_2O_2)
	1943.28 mm (10000 PPM O_3)
CJ - ZND Induction Length	1.04 mm (No Additive)
	0.32 mm (10000 PPM H_2O_2)
	0.29 mm (10000 PPM O_3)

2.2. Boundary and Initial Conditions:

Figure 1 also shows the boundary conditions used for all the simulations. The left boundary is used as the inflow boundary condition with appropriate pressure, temperature and inflow speed along with the species are assigned for the same as shown in Table1. The freestream pressure of 20 kPa and temperature of 300K have been used for all the simulations with a fixed wedge angle of 26°. All the time-dependent simulations are initialized with impulse start and stopped at 100 μs, which is found sufficient time interval for stable oblique shock wave or oblique detonation wave formation. The end solution was analysed for abrupt and smooth transition pattern as well as initiation length for oblique shock to detonation wave transition. The careful choice of Mach number, freestream pressure, and temperature conditions, result in the selection of a domain (wedge length) to perform the simulation with adequate grid resolution for the available resources.

2.3. Grid Independence

To perform the grid independence test, two cases at Mach 7 (with 10000 PPM H_2O_2 addition) and Mach 9 (with 10000 PPM O_3) have been selected, representing abrupt and smooth transitions of ODW, respectively. At a freestream Pressure of 20 kPa and a temperature of 300K with a stoichiometric H_2- Air mixture, the CJ conditions are tabulated in Table 1 with a CJ-ZND induction length of 1.04 mm. The addition of H_2O_2 and O_3 in

the mixture further reduces the CJ-ZND induction length to 0.32 mm and 0.29 mm, respectively. However, the change in CJ speed is less than 0.01 % for the mixture with moderate additives, also tabulated in Table 1. It is recommended to use high grid resolution up to 16-64 grid point within the reaction zone for normal detonation simulations. However, Choi et al. [40] and Verreault [41] have obtained grid independent oblique detonation wave transition with 5 to 13 grid points, respectively within the half reaction length. To obtain adequate grid resolution for abrupt and smooth OSW to ODW transitions, three base grids with 4 levels of adaptive grid refinements have been considered for both additive cases of Mach 7 and 9. The base grid with a uniform size of 0.4 mm (coarse), 0.2 mm (medium) and 0.1 mm (fine) have been used for all grid independence cases. The same adaptive grid refinement approach was used with 4 levels: (2, 2, 2, 4), where the minimum grid size will be $1/16^{th}$ of the base grid. The criterion for adaptive grid resolution is used based on the threshold of pressure and density $\varepsilon_p = 40000$, $\varepsilon_\rho = 0.03$. The mass fraction of the main and intermediate species were also considered for adaptive grid refinement as: $\varepsilon_{H_2} = 0.012$, $\varepsilon_{O_2} = 0.1$, $\varepsilon_{H_2O} = 0.085$, $\varepsilon_H = 0.002$, $\varepsilon_O = 0.005$, and $\varepsilon_{OH} = 0.013$. These threshold conditions remained unchanged for all the base grid simulations. Figure 2 shows

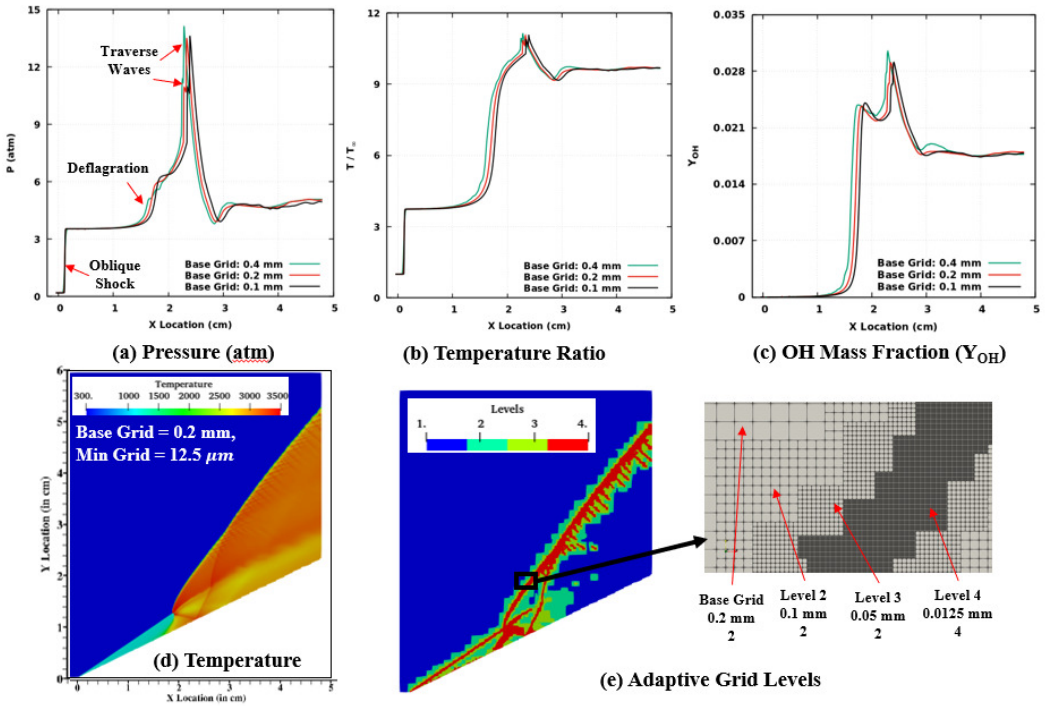

Figure 2. Mach 7 with 10000 PPM H_2O_2 addition: (a) Pressure, (b) Temperature and (c) OH Mass fraction variation at line parallel to wedge for all three grids; (d) Temperature and (e) Adaptive grid levels for medium grid

results from the grid independence study performed for freestream Mach 7 for H_2 and air mixture with a 10000 PPM H_2O_2 addition. Figure 2a, 2b and 2c show the variation in pressure, temperature and OH mass fraction along the line parallel to the wedge length (with a 0.2 mm shift). Figure 2d shows the temperature contours for abrupt transition of the established detonation wave and Fig. 2e shows the used adaptive grid refinement levels (up to 4) in the simulation for a medium grid. The pressure curve in Fig. 2a shows the sudden rise in the pressure near the wedge tip, representing the oblique shock wave and the second rise due to ignition and deflagration wave in the compressed region . The next jumps are representing the traverse waves in abrupt transition. A similar profile is also seen for temperature variation along the wedge in Fig. 2b. The variation in OH mass fraction represent the chemical activity, while pressure and temperature variations represents the gasdynamics structures captured through numerical simulation. All three base grid solu-

tions are able to capture the gas dynamic features of abrupt oblique detonation waves from pressure and temperature curves as well as chemical activity from the OH mass fraction curve. The coarse grid (base grid 0.4 mm) shows a slightly early rise in the deflagration and detonation zones, but medium and fine grids have shown similar initiation structures, without significant difference in the gas dynamic and chemical effects. Hence, medium grid (base grid 0.2 mm) is selected for all the calculations. The temperature contours are shown in Fig. 2d, which clearly captures the oblique shock and abrupt transition through the deflagration zone, triple point, traverse wave, slip line and reflected traverse wave as well as detonation pattern. Fig. 2d shows the 4 levels of adaptive grid refinement used at time $t = 100\mu s$. The used adaptive refinement criteria based on pressure and density as well as species found to be adequate to capture the main features of ODW abrupt transition. The representation of different levels of refinements are shown in the zoomed image in Fig. 2e. The minimum grid size for medium grid (base grid 0.2 mm) with level 4 adaptive grid refinement is 12.5 μm, which represents approximately 25 grid points in the CJ - ZND induction length for 10000 PPM H_2O_2 addition. Although, with overdriven detonation wave at higher Mach numbers, the ZND induction length will be smaller than the CJ-ZND induction length. However within the scope of the study all three grid resolutions are able to capture the required detailed to estimate ODW initiation length and pattern adequately. Moreover, another deciding factor for choosing medium grid solution was computation cost. The single medium grid solution uses approximately 2800 core-hours, while fine grid solution used approximately 12000 core-hours.

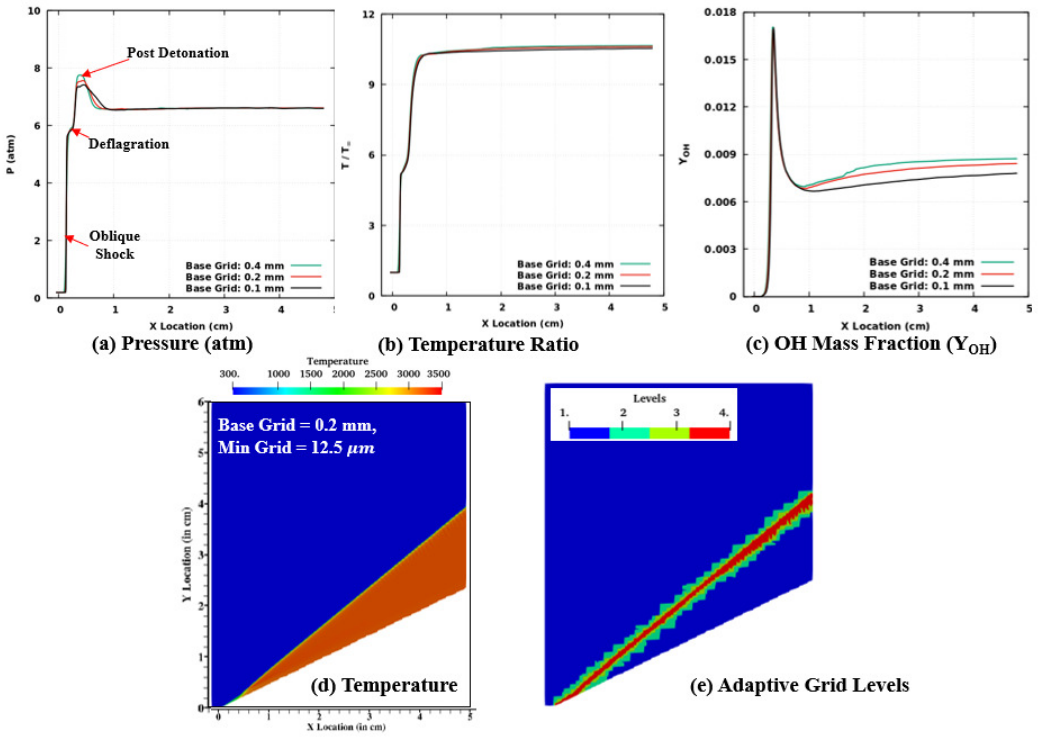

Figure 3. Mach 9 with 10000 PPM O_3 addition: (a) Pressure, (b) Temperature and (c) OH Mass fraction variation at line parallel to wedge for all three grids; (d) Temperature and (e) Adaptive grid levels for medium grid

Further to validate the grid independent solution for smooth transition, the three grid simulations are performed at freestream Mach 9 for H_2 and air mixture with 10000 PPM O_3 addition, shown in Fig. 3. The variation in pressure, temperature and OH mass fraction along the line parallel to the wedge length (with a 0.2 mm shift) are shown in Figure 3a, 3b and 3c. Figure 3d shows the temperature contours for smooth transition and Fig. 3e shows the adaptive grid refinement levels (up to 4) used in the simulation for a medium grid. All

three grids are able to adequately capture the gas dynamics features of smooth transition as different rises in pressure and temperature curves (Fig. 3a and 3b), representing oblique shock wave, deflagration zone and smooth transition to detonation. Also, all three grids, are able to capture the reaction zone, shown as the first peak in OH mass fraction variation (Fig. 3c). However, in the post detonation region, there is small difference in the OH mass fraction along the wedge. Figure 3c shown the temperature contours for smooth transition and Fig. 3e shows the level 4 adaptive grid refinement used for smooth transition. The main objectives of this study is to differentiate between abrupt and smooth transition of ODW and quantify the effect of H_2O_2 and O_3 addition on initiation length of OSW to ODW transition. The grid independence study concludes that it is adequate to use a medium base grid (0.2 mm) and level 4 adaptive grid refinement (minimum grid size 12.5 μm) for all three freestream Mach numbers 7, 8 and 9 and up to 10000 PPM addition of H_2O_2 and O_3.

3. Results & Discussions

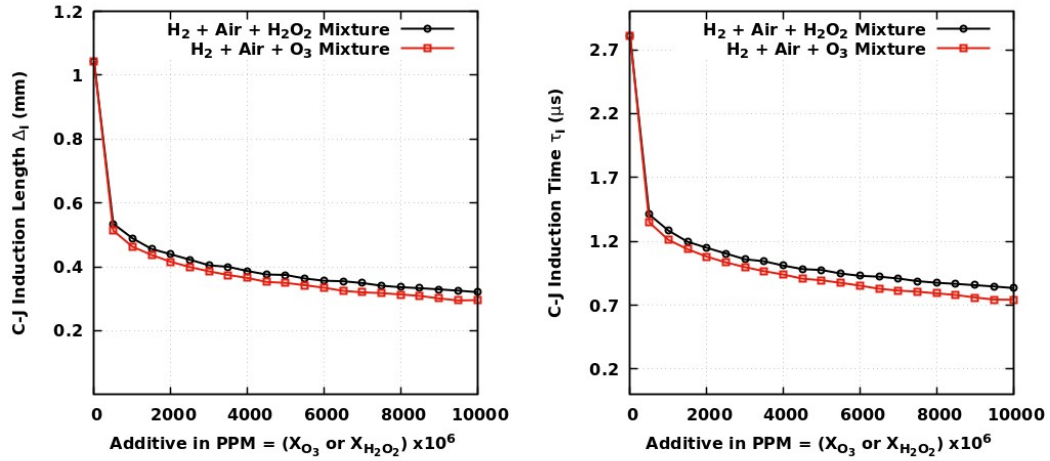

(a) CJ - ZND Induction Length (left) & Induction Time (right) for Different Mixtures

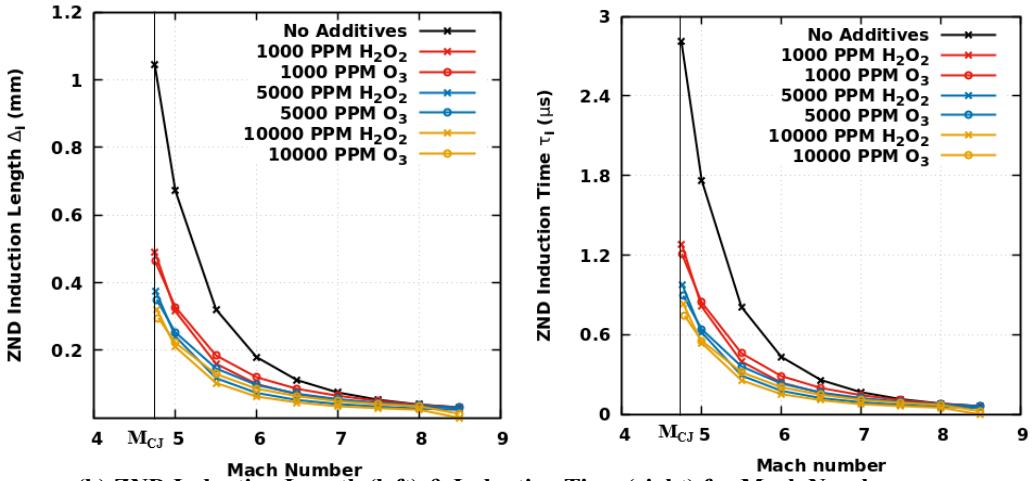

(b) ZND Induction Length (left) & Induction Time (right) for Mach Numbers

Figure 4. Induction Length (Δ_i) and Induction Time (τ_i variation with (a) Additives, Based on CJ - ZND calculation (b) Mach number, Based on overdriven ZND Calculation

The transition pattern of oblique shock to oblique detonation wave highly depends on wedge angle as well as incoming flow speed along with chemical kinetics. It is also well known that low Mach number flow shows abrupt transition for stoichiometric H_2- Air premixed mixture when compared to high Mach number flow. To obtain abrupt to smooth transition for a finite length of wedge, three freestream Mach numbers are selected for a H_2- Air premixed mixture ($\phi = 1$) at fixed freestream pressure of 20 kPa and temperature

300K. In further simulations, the incoming H_2- Air mixture is homogeneously sensitized using H_2O_2 and O_3 additives in moderate amounts to find their effectiveness for ODW formation. In order to estimate the amount of additive required to control the ODW formation, initially ZND calculations are performed to estimate the induction length and induction time using the Shock detonation toolbox [42] based on Cantera [43]. Kumar et al. [18] has previously confirmed using CJ - ZND calculations at 1 atm and 295 K for H_2- Air mixture that the addition of H_2O_2 and O_3 in moderate amount can significantly change the ignition chemistry of the unburned mixture without significantly changing its thermodynamic and physical properties. The ignition promotion by H_2O_2 and O_3 is caused due to reduction in the induction length and induction time because of the shift in the thermicity curve towards the shockwave. Figure 4a shows the variation of the induction zone length and induction time for different amounts of H_2O_2 and O_3 addition. These variations are plotted based on ZND calculations at CJ speeds with the mixture at a pressure of 20 kPa and temperature of 300K. The molar concentration of H_2O_2 and O_3 varied up to 10000 PPM. The variations in CJ speed is less than 0.01 % while varying the amount of additives up to 10000 PPM as the thermodynamic and physical properties of the mixture does not change significantly. The changes in CJ speed with 10000 PPM additives are mentioned in Table 1. With only 1000 PPM of H_2O_2 or O_3 addition, the induction length reduces to 50 % and induction time reduces to 57 %. However, further 10 fold increase in concentration can lead to a further 33 % reduction in induction length and induction time. The effect of Mach number on ZND induction zone length and induction time is also plotted in Fig. 4b along with 1000, 5000 and 10000 PPM H_2O_2 or O_3 addition.The CJ Mach number with no additives is $M_{CJ} = 4.75$ at 20 kPa and 300K, which is marked as a straight vertical line in Fig. 4b. For all the mixtures, with and without additives, an increase in Mach number from M_CJ to 7, leads to 85 - 88 % reduction in induction zone length based on ZND calculations and a similar exponential reduction is observed in induction time. At Mach 9, a ZND solution could not be obtained as the induction length and time become too small. It is noteworthy that the ZND calculation here, which do not represent the wedge stabilized oblique detonation wave, which is a weakly overdriven detonation wave at an angle. ZND model solves one-dimensional steady detonation wave, which assumes frozen chemistry across leading normal shock and postshock the mixture reacts to reach final equilibrium. The above one-dimensional ZND calculations give an indicative estimate to use the amount of additives to influence the induction length and induction time in gaseous detonation. However, the effect of additives on oblique detonation wave structure and its transition characteristics can only be obtained by solving two or three-dimensional equations with detailed chemistry. In the next sections, results from two-dimensional wedge stabilized oblique detonation wave simulations are analyzed for three Mach numbers 7, 8 and 9 up to 10000 PPM H_2O_2 as well as O_3 additives for a finite length wedge. The results are discussed for ODW formation without additives first and then with additives. In order to obtain ODW on a fixed wedge length of 4.8 cm at lower Mach number 7, minimum addition of 1000 PPM H_2O_2 and O_3 is simulated, along with cases with higher addition of 5000 PPM and 10000 PPM H_2O_2 and O_3.

3.1. ODW Formation with no additives

The inflow Mach number affects the abrupt or smooth transition of OSW to ODW. Hence, the initial simulations for pure H_2- Air premixed mixture are performed at three Mach numbers with a fixed wedge angle of 26° and an axial length of 4.8 cm. As the inflow Mach number increases above M_{CJ} for the given premixed mixture, the minimum deflection angle requirement θ_{CJ} rapidly increases [5]. The stoichiometric mixture of H_2- Air at a pressure of 20 kPa and temperature of 300 K has the deflection angle window for stable oblique shock between 15.6° to 39.3° at Mach 7. While conducting the initial simulation at Mach 7 the axial length of 4.8 cm of wedge was not found to be sufficient to establish ODW. Hence, in this particular case at Mach 7, the axial wedge length was increased to 10.8 cm with a domain size of 11 × 10 cm, without changing the adopted grid

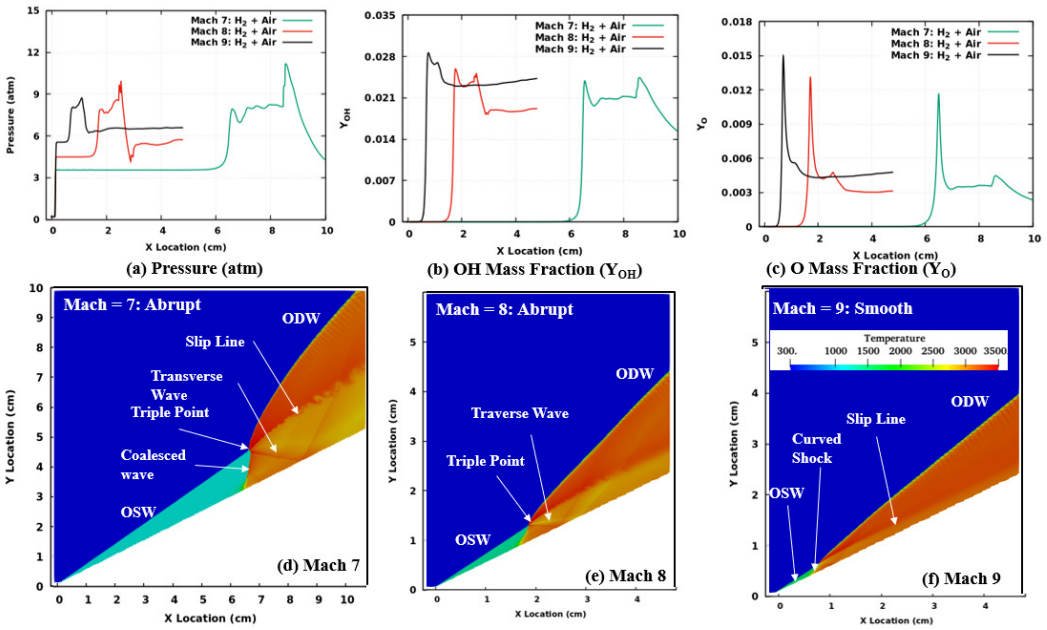

Figure 5. (a) Pressure (b) O Mass Fraction, and (c) OH Mass Fraction variation along the wedge surface and Temperature contours for (d) Mach 7, (e) Mach 8 and (f) Mach 9 freestream flow without additives.

resolution to obtain the abrupt transition of OSW to ODW as shown in Fig 5d. All other cases, even with H_2O_2 and O_3 additives at Mach 7 are simulated with 4.8 cm axial length wedge size. It can be assumed that there is no ODW formation at Mach 7 for 4.8 cm axial wedge length. However, the wedge length was increased to confirm that the selected finite wedge length was not sufficient to establish ODW at Mach 7, even the deflection angle was 10° higher than θ_{CJ} at Mach 7. Figure 5a shows the pressure variation along a line parallel to the wedge (with a 0.2 mm shift). Along the line, the first pressure jump occurs near the wedge tip due to non-reactive OSW. The shock related pressure jump increases with an increase in Mach number due to higher compression. At a further axial distance, the pressure jumps again near the initiation zone of ODW and both the curves at Mach 7 and 8 consist of ripples due to abrupt ODW transition because of the presence of transverse wave and reflected waves. At Mach 9, OSW to ODW transition occur due to smooth curved shock and the pressure curve shows smooth single peak near the initiation zone. Figure 5b and 5c shows the OH and O mass fraction along the wedge surface, reflecting the chemical activity near the initiation and flame zone. The two peaks in OH (Fig. 5b) and O (Fig. 5c) mass fractions are corresponding to initial coalesced and downstream traverse waves. With an increase in Mach number, ODW transition pattern changes from abrupt to smooth transition and the gap between these two peaks decreases or the second peak becomes a plateau, due to the non-existence (or weakening) of traverse waves in smooth transition.

Table 2. Comparison of Theoretical and Numerical ODW Angles (No Additives)

Mach Number	Theoretical ODW Angle	Numerical ODW Angle
Mach =7	47.7°	47.1°
Mach =8	42.5°	44.9°
Mach =9	39.2°	38.9°

Various flow features are mentioned for Mach 7 and Mach 8 abrupt transition and Mach 9 smooth transition in Fig. 5d, 5e, 5f. At Mach 7 abrupt transition, the triple point separates OSW and ODW and the front coalesced wave and traverse wave forms a $\lambda-$ shape shock pattern. An unstable slip line with roll-up behavior of the K-H instability in the detonation zone, along with a reflected traverse wave is also captured at abrupt transition.

The simulations also show detonation cell-like structures in ODW. Qualitatively, the above numerical simulation result at Mach 7 captures non-reactive initiation zone, deflagaration waves, and oblique detonation wave experimentally visualized by Viguier [4]. Recently, Zhang et al. [44] has also reported much clear experimental flow feature captured from ODWE model experiment in hypersonic wind tunnel (M_∞ = 6.6) with the abrupt transition was termed as strong ODW mode. The oblique detonation wave forms as oblique Mach stem due to confined space. These results confirm presence of triple point and transverse wave in experiment, similar to flow feature obtained in above numerical simulation in Fig. 5d. At Mach 8 (Fig. 5e) also, abrupt transition is observed with triple point dividing the OSW and ODW, and with weaker coalesced and traverse waves (than Mach 7) behind the initiation zone. The angle of ODW has been reduced at the higher Mach number 8 when compared to Mach 7. At Mach 9 (Fig. 5f) the triple point has almost disappeared and smooth transition occurs with curved shock and traverse wave disappearing too, while the slip line behind the initiation zone becomes parallel to the wedge. The weak detonation result reported by Zhang et al. [44] shows smooth transition of OSW to ODW transition with absence of tripple point and formation of series of compression waves transiting to Oblique detonation wave. The similar flow features are observed in smooth transition obtained at Mach 9 (in Fig. 5f), qualitatively. The oblique detonation wave angle becomes smaller in weak (smooth transition) ODW mode than the strong (abrupt transition) ODW mode in experiments. Table 2 compares the theoretical and numerical ODW angles for simulated conditions. The theoretical ODW angle are obtained assuming post shock equilibrium conditions with $M - \beta - \theta$ relation and fixed wedge angle (θ =) 26°. At Mach 7 and Mach 9, the ODW angles matches well with theoretical values, however, there is small difference in theoretical and numerical ODW angles. It is evident here that OSW to ODW transition may occur abruptly at lower Mach numbers for fixed wedge angle and premixed mixture. However the high Mach numbers show smooth transition with a smaller initiation length. The initiation length is quantified here from the intermediate O atom peaks along the wedge surface. The axial initiation length at Mach 7 is observed as 6.5 cm (beyond 4.8 cm wedge) and it is estimated as 1.70 cm and 0.69 cm at Mach 8 and 9, respectively. In the next sections, the effect of chemistry is evaluated on OSW to ODW transition by adding H_2O_2 and O_3 up to 10000 PPM in premixed H_2- Air mixture (at $\phi = 1$).

3.2. *Effect of* H_2O_2 *and* O_3 *addition at Mach 7*

The preliminary ZND calculations for CJ speed in Figure 4 show that small amount as 1000 PPM addition of H_2O_2 and O_3 can significantly reduce the induction zone length and induction time by ignition promotion. On one hand, Ozone can be easily decomposed into O_2 and O atom at all concentration levels by the third body reaction. The O atom in the induction zone accelerates the chain branching process, which leads to reduction in ignition time delay. On the other hand, hydrogen peroxide can be readily decomposed into 2 hydroxyl OH radicals by third body reaction, leading to rapid temperature rise and reduction in ignition time-delay. At Mach 7, we can assume that a wedge with a finite axial length of 4.8 cm, could not establish the ODW (the axial initiation length is 6.5 cm as shown with the larger domain simulation in the previous section 3.1). The numerical simulations are performed for 1000, 5000 and 10000 PPM addition of H_2O_2 and O_3 at this Mach number. In order to understand the chemical effect of additives on ODW formation, the mass fraction of intermediate species O and OH are plotted along the wedge axial length in Fig. 6b and 6c. Pressure variation along the wedge (Fig. 6a) and temperature (Fig. 6d) and pressure contours (Fig. 6e) are plotted to understand the gasdynamics effects. With the small amount (1000 PPM) addition of O_3 and H_2O_2, the oblique detonation wave stabilizes on a finite length wedge with a 2.45 cm axial initiation length (62 % reduction). Both O_3 and H_2O_2 addition shows similar profiles to O and OH mass fraction variation in Fig. 6b and 6c. However, the OSW to ODW transition remains abrupt in nature with a $\lambda-$ shock pattern for both additive cases of 1000 PPM O_3 and H_2O_2, which is clearly reflected as double peaks in pressure, OH and O mass fraction plots as well as temperature and

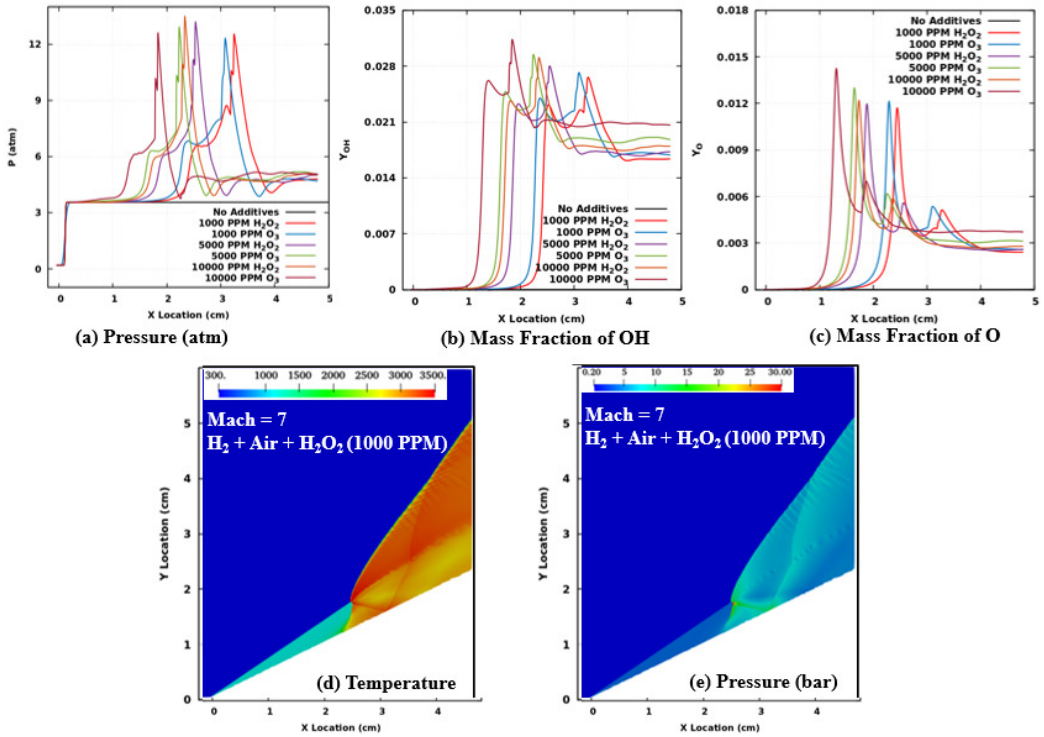

Figure 6. (a) Pressure, (b) OH Radical Mass fraction, (c) O variation along the wedge surface, and (d) Temperature, and (e) Pressure Contour for 1000 PPM H_2O_2 addition at Mach 7

pressure contours for 1000 PPM H_2O_2 addition. The further addition of 5000 and 10000 PPM additives, reduces the initiation length to establish the ODW, but the nature of the transition does not change. The intermediate species mass fraction as well as pressure curves show similar profiles but a shift in the axial direction. The higher additions of O_3 and H_2O_2 show slight difference in their effectiveness. The O_3 addition further reduces the initiation length in comparison to the same amount of H_2O_2 addition. It can be understood that O_3 decomposition is prevalent even at lower compressed temperature and pressure (in comparison with higher Mach numbers) after the oblique shock at Mach 7, while the OH formation increases at upstream location on the wedge (2^{nd} peak is higher in OH profile). H_2O_2 may require a higher temperature to decompose into OH. Additionally, O_3 can also increase O_2 concentration near the end of the initiation length which can significantly promote reactivity in the compressed region.

3.3. Effect of H_2O_2 and O_3 addition at Mach 8

The ODW formation at Mach 8 shows features of abrupt OSW to ODW transition in Fig. 5e with triple point, transverse wave slipline, reflected transverse wave etc. However, a steeper detonation wave angle can be observed at Mach 8 when compared to lower Mach number 7. Figure 7 shows the chemical and gasdynamics effects of 1000, 5000, and 10000 PPM H_2O_2 and O_3 addition at Mach 8 ODW transition. A small amount of 1000 PPM can significantly reduce the initiation length on the wedge. It is observed that 1000 PPM H_2O_2 addition is more effective in reducing the initiation length than the same amount of O_3 addition. The pressure variation, which shows ripples after the second jump due to a abrupt shock pattern without any additive, becomes smoother with 1000 PPM H_2O_2 addition, suggesting a change in abrupt to smooth OSW to ODW transition. The mass fraction of intermediate species OH (Fig. 7b) and O (Fig. 7c), shows two peaks in the no additive case, the downstream peak disappears or modifies to plateau with an increase in additive amounts, due to a disappearing or weakening traverse wave. The OH mass fraction shows first peak higher than the second peak (opposite to Mach 7 case in Fig 6a),

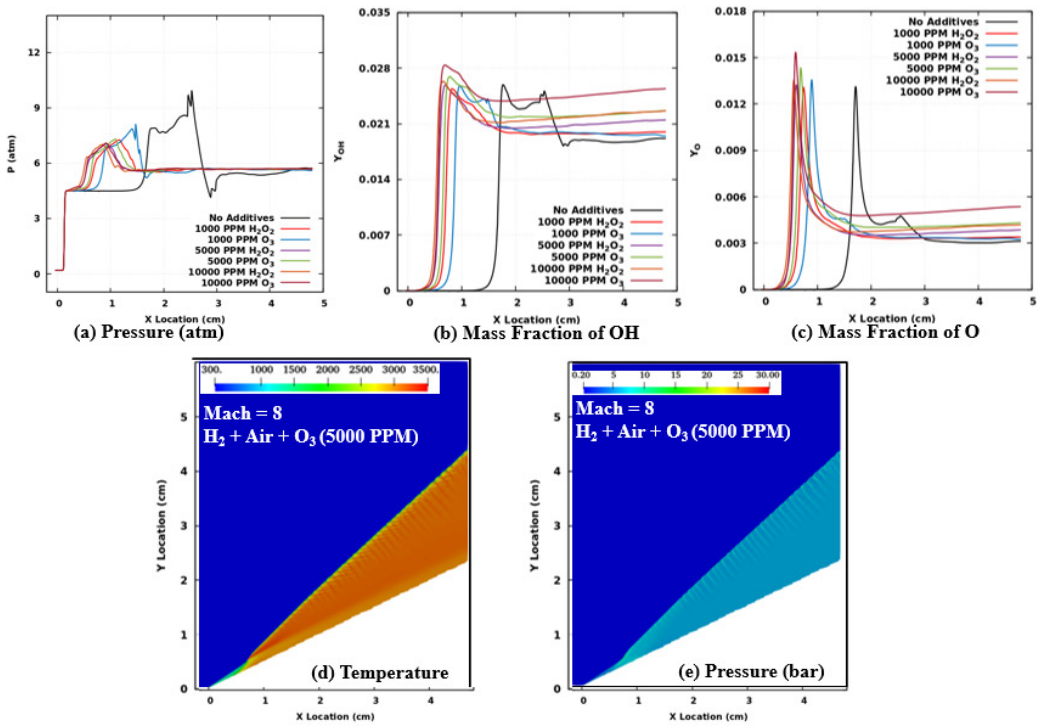

Figure 7. (a) Pressure, (b) OH Radical Mass fraction, (c) O variation along the wedge surface, and (d) Temperature, and (e) Pressure Contour for 5000 PPM O_3 addition at Mach 8

suggesting that H_2O_2 decomposition becomes dominant to increase the reactivity after the Mach 8 compressed oblique shock. The OH dominant ignition promotion rapidly increases the temperature in a smaller zone, may benefit a smooth transition of ODW formation. The temperature (Fig. 7d) and pressure (Fig. 7e) for 5000 PPM O_3 addition shows features of smooth OSW to ODW transition such as the curved shock, a disappearance of the transverse wave and slip line parallel to wedge. Furthermore, a 10000 PPM addition of H_2O_2 and O_3 leads to OSW to ODW transition closer to the wedge tip with no significant reduction in initiation length as compared to the addition of 1000 PPM. However H_2O_2 addition is still marginally effective than compare to same amount of O_3 addition. As the OSW to ODW transition at Mach 8 is moderately abrupt in case of no additive, the addition of an ignition promoter can change the transition pattern from abrupt to smooth with a rapid increase in temperature and reduction in the initiation length.

3.4. Effect of H_2O_2 and O_3 addition at Mach 9

The OSW to ODW transition at Mach 9 is smooth in nature. Figure 8 shows the variation of pressure and intermediate species the mass fractions near the wedge surface parallel line and the temperature, pressure contours for the 1000 PPM O_3 addition. For the no additive case at Mach 9, in Fig. 4d, the OSW to ODW smooth transition occurs at the 0.78 cm axial distance, which also shows the curved shock and no triple point formation with the slip line parallel to the wedge. The pressure and intermediate species variation in Fig. 7a - 7c shows a smooth single peak in the reaction zone for the no additive case. The small 1000 PPM addition of H_2O_2 and O_3 additives, shifts the reaction zone towards the wedge tip, with the H_2O_2 addition leading to a higher initiation length reduction when compared to the same amount of O_3 addition. As H_2O_2 decomposition occurs at slightly elevated temperatures when compared to O_3 decomposition, the highly compressed region behind the oblique shock at the higher Mach number can provide favourable conditions for H_2O_2 decomposition. A further rapid increase in temperature due to OH formation can facilitate the smooth transition of OSW to ODW formation. The increase in H_2O_2 and O_3 addition to 5000 PPM and 10000 PPM further reduces the initiation length and moves

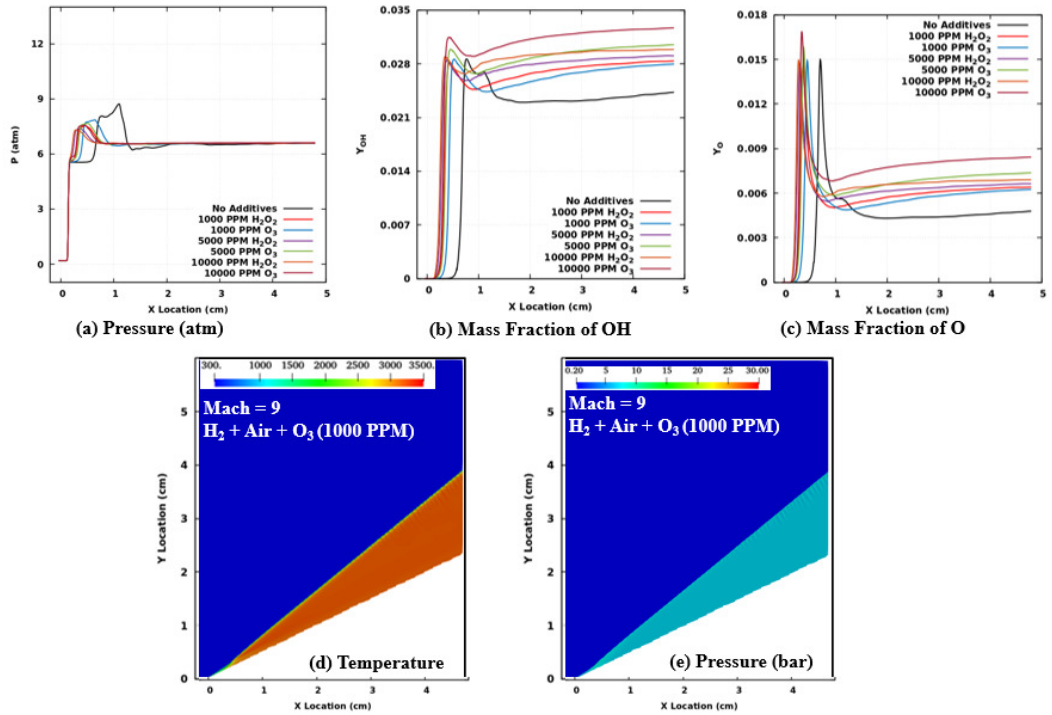

Figure 8. (a) Pressure, (b) OH Radical Mass fraction, (c) O variation along the wedge surface, and (d) Temperature, and (e) Pressure Contour for 1000 PPM O_3 addition at Mach 9

the transition region closer to the wedge tip. The effectiveness of the H_2O_2 addition is still better for initiation length reduction than the same amount of O_3 addition at higher PPM. The temperature and pressure contours of 1000 PPM O_3 addition shows no significant change in ODW angle when compared to the no additive case (Fig. 5f).

3.5. Effect on ODW Initiation Length

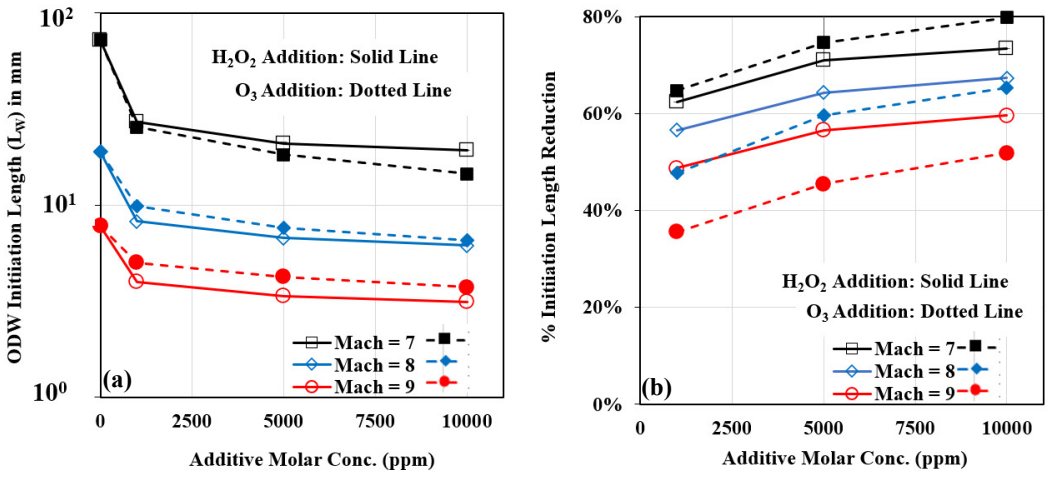

Figure 9. Initiation Length variation with additives at H_2- Air ($\phi = 1$ premixed mixture

Figures 9a and 9b quantify the effectiveness of H_2O_2 and O_3 addition on ODW initiation length control. The initiation length (L_w) is defined as the length along the wedge surface, when the peak oxygen atom (O) mass fraction occurs. The axial X distance is converted to the initiation length with use of simulated wedge angle of $\theta = 26°$. In the case of no additives, the initiation lengths computed are 7.2 cm, 1.89 cm, and 0.78 cm for Mach 7, 8 and 9 cases, respectively. In case of Mach 7, the ODW formation occurs beyond the finite wedge length (of 4.8 cm) used in the current study. As the Mach number increases

from 7 to 9, the OSW to ODW transition moves from abrupt to moderately abrupt and to a smooth transition, moving towards the wedge tip. With the increase in Mach number for a fixed wedge angle, the compression by initial OSW in the initiation zone increases the pressure and temperature near the wedge tip and the oblique shock becomes closer to the wedge surface. With the higher pressure and temperature after the oblique shock the fuel-air mixture can achieve the ignition closer to the wegde tip and lead to an abrupt to smoother transition. Figure 9b also shows the percentage reduction in initiation length by use of a small and moderate amount of H_2O_2 and O_3 additives. It can be observed that with a small amount of 1000 PPM, the initiation length is significantly reduced at lower Mach 7 by approximately 62.3 %, with a further increase in additive content, a O_3 addition of 10000 PPM can lead to maximum initiation length reduction of 80 %, while 10000 PPM of H_2O_2 addition can reduce the initiation length by 73%. At higher Mach numbers, it can be seen that H_2O_2 performs well in reducing the initiation lengths in comparison to the same amount of O_3. It can be concluded that H_2O_2 provides better performance in reducing the initiation length at higher Mach numbers or near the smooth OSW to ODW transition operation, while O_3 is a very effective ignition promoter at the lower Mach number range and O_3 can be helpful to increase the lower operating flight speed in detonation mode with a very small addition.

4. Conclusions

The effect of ignition promoters on wedge induced oblique detonation wave formation was investigated by using two-dimensional compressible reactive flow simulations. The H_2-Air premixed incoming flow with and without H_2O_2 and O_3 addition are simulated at three hypersonic Mach numbers 7, 8 and 9 in front of a finite length wedge. From the obtained results, the following can be concluded:

1. The mixing of H_2O_2 and O_3 from a small amount of 1000 PPM to a moderate amount 10000 PPM, can effectively reduce the initiation lengths of oblique shock to oblique detonation wave transition at all Mach 7-9 numbers studied.
2. At Mach 7, the reduction in initiation length is up to 80% with H_2O_2 and O_3 addition during the abrupt transition. The O_3 addition has been found to be more effective in comparison to the H_2O_2 addition at low Mach number abrupt transition condition and it can be utilized to increase lower operating flight speeds for ODWE.
3. At Mach 8, the moderate abrupt OSW to ODW transition can be modified to a smoother transition by adding a small amount of H_2O_2 and O_3. Furthermore, H_2O_2 addition has been found to be more effective in reducing the initiation length in comparison to the same amount of O_3 addition for Mach 8 & 9 during smooth ODW transitions.
4. The Mach number dependence of the compressed region in the initiation zone behind the oblique was responsible for the different performances of H_2O_2 and O_3 addition for initiation length reduction. O_3 decomposition was dominated regarding the initiation length reduction at relatively lower Mach number, while OH formation from H_2O_2 was dominant at higher Mach numbers.

Author Contributions: Conceptualization, A.V.; methodology and solver: R.D.; mechanism integration, S.P.; simulations: A.V., D.C1.; formal analysis and investigation, A.V., S.P.; resources: D.C2. and C.N.; writing—original draft preparation, A.V.; writing—review and editing, A.V., S.P, D.C2., C.N. and R.D. All authors have read and agreed to the published version of the manuscript.

Acknowledgments: The authors would like to acknowledge the Irish Centre for High-End Computing (ICHEC) for the provision of computing resources for this study.

Conflicts of Interest: The authors declare no conflict of interest.

References

1. Lee, J.H.S. *The Detonation Phenomenon*, 1 ed.; Cambridge University Press: Cambridge, 2008. doi:10.1017/CBO9780511754708.

2. Kailasanath, K. Review of Propulsion Applications of Detonation Waves. *AIAA Journal* **2000**, *38*, 1698–1708. doi:10.2514/2.1156.
3. Wolanski, P. Detonative propulsion. *Proceedings of the Combustion Institute* **2013**, *34*, 125–158. doi:10.1016/j.proci.2012.10.005.
4. Viguier, C.; da Silva, L.F.F.; Desbordes, D.; Deshaies, B. Onset of oblique detonation waves: Comparison between experimental and numerical results for hydrogen-air mixtures. *Symposium (International) on Combustion* **1996**, *26*, 3023–3031. doi:10.1016/S0082-0784(96)80146-9.
5. Pratt, D.T.; Humphrey, J.W.; Glenn, D.E. Morphology of standing oblique detonation waves. *Journal of Propulsion and Power* **1991**, *7*, 837–845. doi:10.2514/3.23399.
6. Powers, J.M.; Stewart, D.S. Approximate solutions for oblique detonations in the hypersonic limit. *AIAA Journal* **1992**, *30*, 726–736. doi:10.2514/3.10978.
7. Wang, A.F.; Zhao, W.; Jiang, Z.L. The criterion of the existence or inexistence of transverse shock wave at wedge supported oblique detonation wave. *Acta Mechanica Sinica* **2011**, *27*, 611–619. doi:10.1007/s10409-011-0463-7.
8. Verreault, J.; Higgins, A.J. Initiation of detonation by conical projectiles. *Proceedings of the Combustion Institute* **2011**, *33*, 2311–2318. doi:10.1016/j.proci.2010.07.086.
9. Rosato, D.A.; Thornton, M.; Sosa, J.; Bachman, C.; Goodwin, G.B.; Ahmed, K.A. Stabilized detonation for hypersonic propulsion. *Proceedings of the National Academy of Sciences* **2021**, *118*, e2102244118. doi:10.1073/pnas.2102244118.
10. Silva, F.D.; Deshaies, B. Stabilization of an oblique detonation wave by a wedge: a parametric numerical study. *Combustion and Flame* **2000**, *121*, 152–166. doi:10.1016/S0010-2180(99)00141-8.
11. Teng, H.; Zhang, Y.; Jiang, Z. Numerical investigation on the induction zone structure of the oblique detonation waves. *Computers & Fluids* **2014**, *95*, 127–131. doi:10.1016/j.compfluid.2014.03.001.
12. Zhang, Y.; Yang, P.; Teng, H.; Ng, H.D.; Wen, C. Transition Between Different Initiation Structures of Wedge-Induced Oblique Detonations. *AIAA Journal* **2018**, *56*, 4016–4023. doi:10.2514/1.J056831.
13. Teng, H.; Ng, H.D.; Jiang, Z. Initiation characteristics of wedge induced oblique detonation waves in a stoichiometric hydrogen air mixture. *Proceedings of the Combustion Institute* **2017**, *36*, 2735–2742. doi:10.1016/j.proci.2016.09.025.
14. Gao, Y.; Li, H.; Xiang, G.; Peng, S. Initiation characteristics of oblique detonation waves from a finite wedge under argon dilution. *Chinese Journal of Aeronautics* **2021**, *34*, 81–90. doi:10.1016/j.cja.2020.11.013.
15. Miao, S.; Zhou, J.; Lin, Z.; Cai, X.; Liu, S. Numerical Study on Thermodynamic Efficiency and Stability of Oblique Detonation Waves. *AIAA Journal* **2018**, *56*, 3112–3122. doi:10.2514/1.J056887.
16. Magzumov, A.E.; Kirillov, I.A.; Rusanov, V.D. Effect of small additives of ozone and hydrogen peroxide on the induction-zone length of hydrogen-air mixtures in a one-dimensional model of a detonation wave. *Combustion, Explosion and Shock Waves* **1998**, *34*, 338–341. doi:10.1007/BF02672728.
17. Crane, J.; Shi, X.; Singh, A.V.; Tao, Y.; Wang, H. Isolating the effect of induction length on detonation structure: Hydrogen–oxygen detonation promoted by ozone. *Combustion and Flame* **2019**, *200*, 44–52. doi:10.1016/j.combustflame.2018.11.008.
18. Kumar, D.S.; Ivin, K.; Singh, A.V. Sensitizing gaseous detonations for hydrogen / ethylene-air mixtures using ozone and H_2O_2 as dopants for application in rotating detonation engines. *Proceedings of the Combustion Institute* **2021**, *38*, 3825–3834. doi:10.1016/j.proci.2020.08.061.
19. Qin, Q.; Zhang, X. Nitrogen dilution effects on the local detachment of the oblique detonation wave in the 2H2–O2 mixture. *International Journal of Hydrogen Energy* **2021**, *46*, 6873–6884. doi:10.1016/j.ijhydene.2020.11.157.
20. Zhang, Y.; Fang, Y.; Ng, H.D.; Teng, H. Numerical investigation on the initiation of oblique detonation waves in stoichiometric acetylene–oxygen mixtures with high argon dilution. *Combustion and Flame* **2019**, *204*, 391–396. doi:10.1016/j.combustflame.2019.03.033.
21. Maeda, S.; Inada, R.; Kasahara, J.; Matsuo, A. Visualization of the non-steady state oblique detonation wave phenomena around hypersonic spherical projectile. *Proceedings of the Combustion Institute* **2011**, *33*, 2343–2349. doi:10.1016/j.proci.2010.06.066.
22. Viguier, C.; Gourara, A.; Desbordes, D. Three-dimensional structure of stabilization of oblique detonation wave in hypersonic flow. *Symposium (International) on Combustion* **1998**, *27*, 2207–2214. doi:10.1016/S0082-0784(98)80069-6.
23. Sosa, J.; Rosato, D.A.; Goodwin, G.B.; Bachman, C.L.; Oran, E.S.; Ahmed, K.A. Controlled detonation initiation in hypersonic flow. *Proceedings of the Combustion Institute* **2021**, *38*, 3513–3520. doi:10.1016/j.proci.2020.09.014.

24. Li, C.; Kailasanath, K.; Oran, E.S. Detonation structures behind oblique shocks. *Physics of Fluids* **1994**, *6*, 1600–1611. doi:10.1063/1.868273.
25. Li, C.; Kailasanath, K.; Oran, E., Effects of boundary layers on oblique-detonation structures. In *31st Aerospace Sciences Meeting*; AIAA, 1993; chapter AIAA-93-0450, p. 13. doi:10.2514/6.1993-450.
26. Oran, E.S.; Weber, J.W.; Stefaniw, E.I.; Lefebvre, M.H.; Anderson, J.D. A Numerical Study of a Two-Dimensional H2-O2-Ar Detonation Using a Detailed Chemical Reaction Model. *Combustion and Flame* **1998**, *113*, 147–163. doi:10.1016/S0010-2180(97)00218-6.
27. Deiterding, R. Parallel adaptive simulation of multi-dimensional detonation structures. PhD thesis, Brandenburgische Technische Universitat Cottbus, 2003.
28. Deiterding, R. High-Resolution Numerical Simulation and Analysis of Mach Reflection Structures in Detonation Waves in Low-Pressure H_2–O_2–Ar Mixtures: A Summary of Results Obtained with the Adaptive Mesh Refinement Framework AMROC. *Journal of Combustion* **2011**, *2011*, 738969. doi:10.1155/2011/738969.
29. Deiterding, R. A parallel adaptive method for simulating shock-induced combustion with detailed chemical kinetics in complex domains. *Computers & Structures* **2009**, *87*, 769–783. Fifth MIT Conference on Computational Fluid and Solid Mechanics, doi:10.1016/j.compstruc.2008.11.007.
30. Harmon, P.; Vashishtha, A.; Callaghan, D.; Nolan, C.; Deiterding, R., Study of Direct Gas Injection into stagnation zone of Blunt Nose at Hypersonic Flow. In *AIAA Propulsion and Energy 2021 Forum*; AIAA, 2021; chapter Session:, p. 3529. doi:10.2514/6.2021-3529.
31. Vashishtha, A.; Callaghan, D.; Nolan, C.; Deiterding, R. Numerical Investigation of Detonation Propagation Through Small Orifice Holes. *Transactions on Aerospace Research* **2021**, *2021*, 17–33. doi:10.2478/tar-2021-0014.
32. Liu, Y.; Wang, L.; Xiao, B.; Yan, Z.; Wang, C. Hysteresis phenomenon of the oblique detonation wave. *Combustion and Flame* **2018**, *192*, 170–179. doi:10.1016/j.combustflame.2018.02.010.
33. Liu, Y.; Xiao, B.; Wang, L.; Wang, C. Numerical Study of Disturbance Resistance of Oblique Detonation Waves. *International Journal of Aerospace Engineering* **2020**, *2020*. doi:10.1155/2020/8876637.
34. Huang, Y.; Luan, Z.; Li, Z.; Ji, H.; You, Y. Study on the flow characteristics in the non-detonation reaction zones of wedge-induced oblique detonation transitions. *Aerospace Science and Technology* **2022**, *120*, 107282. doi:10.1016/j.ast.2021.107282.
35. Westbrook, C.K. Chemical kinetics of hydrocarbon oxidation in gaseous detonations. *Combustion and Flame* **1982**, *46*, 191–210. doi:10.1016/0010-2180(82)90015-3.
36. Zhao, H.; Yang, X.; Ju, Y. Kinetic studies of ozone assisted low temperature oxidation of dimethyl ether in a flow reactor using molecular-beam mass spectrometry. *Combustion and Flame* **2016**, *173*, 187 194. doi:10.1016/j.combustflame.2016.08.008.
37. Atkins, C.W.C.; Deiterding, R. Modelling Hypersonic Flows in Thermochemical Nonequilibrium Using Adaptive Mesh Refinement. In Proceedings of the 7th European Conference on Computational Fluid Dynamics; , 2018; pp. 672–683. https://eprints.soton.ac.uk/420989/.
38. Scoggins, J.B.; Leroy, V.; Bellas-Chatzigeorgis, G.; Dias, B.; Magin, T.E. Mutation++: MUlticomponent Thermodynamic And Transport properties for IONized gases in C++. *SoftwareX* **2020**, *12*, 100575. doi:10.1016/j.softx.2020.100575.
39. Shi, L.; Shen, H.; Zhang, P.; Zhang, D.; Wen, C. Assessment of Vibrational Non-Equilibrium Effect on Detonation Cell Size. *Combustion Science and Technology* **2017**, *189*, 841–853. doi:10.1080/00102202.2016.1260561.
40. Choi, J.Y.; Kim, D.W.; Jeung, I.S.; Ma, F.; Yang, V. Cell-like structure of unstable oblique detonation wave from high-resolution numerical simulation. *Proceedings of the Combustion Institute* **2007**, *31*, 2473–2480. doi:10.1016/j.proci.2006.07.173.
41. Verreault, J.; Higgins, A.J.; Stowe, R.A. Formation of transverse waves in oblique detonations. *Proceedings of the Combustion Institute* **2013**, *34*, 1913–1920. doi:10.1016/j.proci.2012.07.040.
42. Browne, S.; Ziegler, J.; Bitter, N.; Schmidt, B.; Lawson, J.; Shepherd, J.E. SDToolbox: Numerical Tools for Shock and Detonation Wave Modeling. Technical Report GALCIT Technical Report FM2018.001 Revised January 2021, Explosion Dynamics Laboratory, 2018.
43. Goodwin, D.G.; Speth, R.L.; Moffat, H.K.; Weber, B.W. Cantera: An Object-oriented Software Toolkit for Chemical Kinetics, Thermodynamics, and Transport Processes. https://www.cantera.org, 2021. Version 2.5.1, doi:10.5281/zenodo.4527812.
44. Zhang, Z.; Wen, C.; Yuan, C.; Liu, Y.; Han, G.; Wang, C.; Jiang, Z. An experimental study of formation of stabilized oblique detonation waves in a combustor. *Combustion and Flame* **2022**, *237*, 111868. doi:10.1016/j.combustflame.2021.111868.